Multiple Neural Modules Orchestrate Conflict Processing

Melinda Sabo [1*], Manuel Varlet [2,3], & Tijl Grootswagers [2,4]

[1] Leibniz Research Centre for Working Environment and Human Factors, Dortmund, Germany
[2] The MARCS Institute for Brain, Behaviour and Development, Western Sydney University, Sydney Australia
[3] School of Psychology, Western Sydney University, Australia
[4] School of Computer, Data and Mathematical Sciences, Western Sydney University, Australia

Author Note

Melinda Sabo https://orcid.org/0000-0001-8585-7115
Manuel Varlet https://orcid.org/ 0000-0001-5772-2061
Tijl Grootswagers https://orcid.org/0000-0002-7961-5002

*Correspondence concerning this article should be addressed to Melinda Sabo, Leibniz Research Centre for Working Environment and Human Factors, Ardeystraße 67 44139 Dortmund, Germany
E-mail: melinda.sabo2@gmail.com

Abstract

Cognitive conflict is a ubiquitous aspect of our daily life, yet its underlying neural mechanisms remain debated. Competing theories propose that conflict processing is governed by either a domain-general system, multiple conflict-specific modules, or both types of systems, as evidenced by hybrid accounts. The aim of the current study was to settle this debate. We analyzed electroencephalogram (EEG) data from 507 participants (ages 20–70) who completed three conflict tasks: a change detection, a Simon, and a Stroop task. A novel decoding approach was adopted to distinguish between conflict and non-conflict trials. While within-task decoding showed robust effects, decoding across tasks yielded chance-level evidence. These findings support the idea that conflict processing relies on multiple conflict specific modules tailored to task-specific demands. By leveraging a large, diverse sample and a data-driven analysis, this study provides compelling evidence for conflict-specific neural mechanisms, offering new insights into the nature of conflict resolution and cognitive control.

Keywords: cognitive control, attention, Simon task, Stroop task, decoding, EEG

1. Introduction

In our everyday life, we are constantly exposed to situations where we must overcome conflict. It is often the case that our cognitive system triggers an automatic response, while the situation requires a different, competing response. For example, if someone accustomed to driving in a country where vehicles travel on the left side of the road visits a country where driving occurs on the right side, they might instinctively look in the wrong direction when crossing the street. Overcoming this habitual response requires conscious effort and adjustment. This scenario exemplifies the type of cognitive conflict we must navigate. Such adaptations are made possible through cognitive control, a fundamental mechanism that allows humans to flexibly adjust to the ever-changing demands of the environment.

Conflict processing has been extensively studied in laboratory settings using various experimental paradigms. One prominent example is the Stroop task (Heidlmayr et al., 2020; Parris et al., 2022; Stroop, 1935), where participants are shown a color word (e.g., "red") written in incongruent ink (e.g., blue). Because the color and word meaning are processed simultaneously, the irrelevant word meaning interferes with the display color and leads to conflict. Another well-known paradigm is the Simon task. In this case, participants are required to respond with either the left or right hand based on a symbol's meaning. Conflict arises when the symbol's spatial location (e.g., appearing on the left) does not align with the required response hand (e.g., right hand) (Cespón et al., 2020; Hommel, 2011; Leuthold, 2011; Simon, 1969). Finally, conflict has also been investigated in change detection paradigms, where participants are required to report changes in a specific feature between two successively flashed stimuli (Schneider & Wascher, 2013; Wascher & Beste, 2010). Research across these different experimental paradigms revealed that conflict emerges when task-irrelevant changes are introduced, which compete with the task-relevant feature change, decreasing overall behavioral performance.

The underlying conflict processing and control mechanisms have been and remain the subject of many debates. According to one of the most prominent conflict-monitoring models, the brain manages conflict through a domain-general conflict-control loop (Botvinick et al., 2001). This loop includes a detection module (linked to the anterior cingulate cortex) for identifying conflict and a control module (linked to the prefrontal cortex) for resolving it and coordinating adaptive responses (Gratton et al., 2018). A central assumption of this model is that this mechanism is domain-general, so the same brain regions and networks are active independently of task or conflict type (Botvinick et al., 2001).

While domain-general conflict processing models suggest a unified neural mechanism for conflict detection and control, subsequent findings have called this assumption into question. Emerging research suggests that different types of conflict—such as stimulus-based conflict (e.g., Stroop tasks) and response-based conflict (e.g., Simon tasks)—elicit distinct neural activation patterns. Stimulus-based conflicts are associated with frontal and parietal activation, whereas response-based conflicts engage motor and premotor areas (Cespón et al., 2020; Egner, 2008; H. Li et al., 2019; Parris et al., 2019, 2022; Zmigrod et al., 2016). Behavioral studies further support these findings, suggesting that conflict processing and control frequently depend on task-specific strategies (Blais & Bunge, 2010; Funes et al., 2010; Kim et al., 2010; Scerrati et al., 2017). Together, these studies suggest that the neural mechanisms for conflict resolution may be modular and task-dependent, challenging the domain-general perspective (for a review see, Egner, 2008).

Existing literature thus suggests the emergence of two competing models: one supporting a unified, domain-general mechanism (Botvinick et al., 2001; Kan et al., 2013) and the other advocating for multiple conflict-specific modules (Egner, 2008; Egner et al., 2007; Funes et al., 2010; Kim et al., 2010; Scerrati et al., 2017; Zmigrod et al., 2016). More recently, a hybrid model has also been proposed, suggesting that the brain integrates a general mechanism with specialized sub-modules to handle distinct conflict types (Q. Li et al., 2017). However, the hybrid perspective has been so far only supported by limited evidence, leaving the debate unresolved and highlighting the need for further investigation.

Therefore, the current study seeks to clarify the brain mechanisms underlying conflict processing and control. Specifically, we examine whether conflict processing is governed by (i) a domain-general conflict processing module with a corresponding unified neural mechanism, (ii) multiple highly specialized conflict-specific modules with fully distinct neural mechanisms, or (iii) a hybrid architecture involving both domain-general, as well as conflict-specific sub-modules. To address this question, we leverage a large electroencephalogram (EEG) dataset collected from 507 participants, spanning an age range of 20–70 years, which is representative of the general population. Participants performed three cognitive tasks traditionally associated with conflict processing: a change detection task involving task-relevant and irrelevant features, a Simon task, and a Stroop task (see Figure 1). Notably, while the Stroop task primarily involves stimulus conflict and the Simon involves response conflict, the change detection task introduced in this study incorporates both types of conflict. These three tasks are therefore well-suited not only to evaluate the first two models but also to assess the plausibility of the hybrid model.

Using multivariate pattern analysis, we examine whether a linear classifier can learn to distinguish conflict from non-conflict trials based on EEG data. First, we train a classifier to identify conflict-related patterns within each task. We not only run this analysis in the time domain, but also in the frequency domain, as previous research highlights the role of theta-band activity in conflict processing (Hanslmayr et al., 2008; Nigbur et al., 2011). Next, we investigate whether these conflict signals generalize across tasks by training the classifier on one task (or a combination of tasks) and evaluating its performance on the remaining task, a process referred to as cross-task decoding. In this context, three outcomes are possible. The *domain-general conflict processing perspective* predicts above-chance decoding performance for both within-and cross-task decoding. Alternatively, under the *multiple conflict-specific modules* framework, only within-task decoding is expected to produce statistically reliable results. Finally, the *hybrid model* entails an above-chance decoding accuracy for the within-task procedure, but not for all cross-task decoding combinations. Specifically, we expect above-chance decoding accuracy when pairing the change-detection task with either the Simon or Stroop tasks due to some shared conflict-processing mechanisms. However, given the substantial differences between the Simon and Stroop tasks, cross-task decoding in this case should remain at chance level. To foreshadow our findings, both time-domain and frequency-domain analyses showed that conflict decoding was successful within individual tasks. However, cross-task decoding analyses indicated that the conflict signal did not generalize across tasks, supporting the predictions of the *multiple conflict-specific modules* framework.

2. Results

The current study investigates the neural mechanisms of conflict processing to determine whether they align with a domain-general, conflict-specific, or hybrid model. We recorded EEG data from 507 participants (aged 20–70) during three conflict tasks: a change detection

task, the Simon task, and the Stroop task (Figure 1). While the Simon and Stroop tasks primarily target response-level and stimulus-level conflict, respectively, the change detection task uniquely integrates both. Analyzing such a large and diverse dataset mitigates common challenges in small-sample EEG research, such as low statistical power and noise-related unreliability. Furthermore, our novel cross-task decoding approach avoids assumptions about specific underlying neural components or activation shared across tasks, relying instead on the classifier to detect these regularities. Together, these methodological strengths make our study well-suited to addressing this critical question and providing robust evidence that settles a long-standing debate.

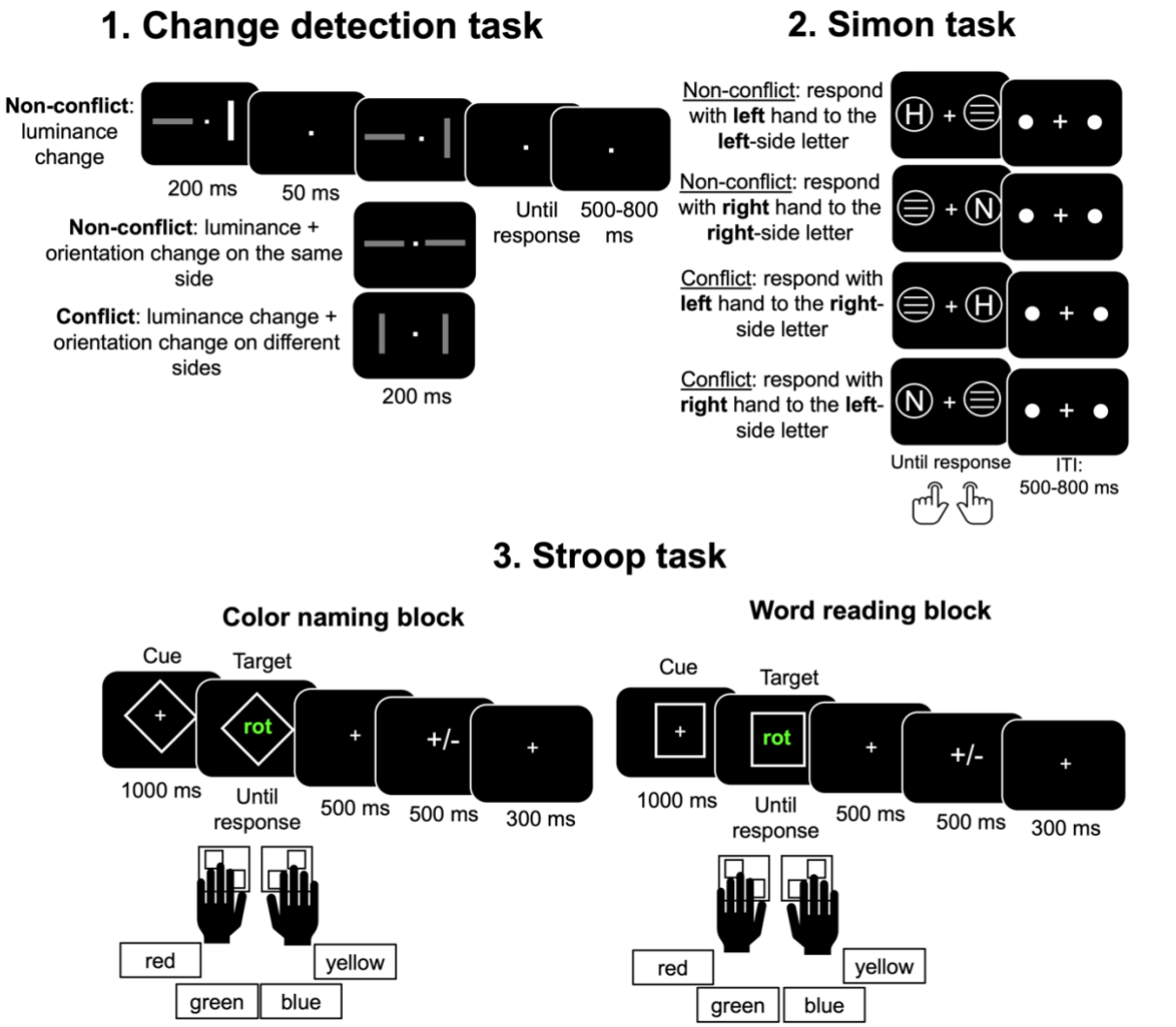

Figure 1. Overview of experimental tasks involving conflict at different levels. (a) Change detection task: Participants viewed two squares on either side of a fixation cross. Stimuli could include a luminance change (non-conflict), a luminance and orientation change on the same side (non-conflict), or a luminance and orientation change on opposite sides (conflict). Participants responded to the change location, with trials separated by an inter-trial interval (ITI) of 500–800 ms. **(b) Simon task**: Participants responded to a letter presented on either side of the screen (H or N) using a spatially compatible or incompatible hand. Non-conflict trials required spatially congruent responses, while conflict trials involved spatially incongruent responses, with an ITI of 500–800 ms. **(c) Stroop task**: Two blocks of trials were included: a **Color Naming Block**, in which participants named the ink color of a word regardless of the word's meaning, and a **Word Reading Block**, in which participants read the word regardless of its ink color. The task included four colors, red, yellow, green, blue, displayed in German (i.e., "rot", "gelb", "grün", "blau"). Responses were made using four keys corresponding to the four possible colors, and each trial began with a cue, followed by the target word and a variable ITI.

2.1.Successful within-task decoding – evidence from the time domain

The first step in our analysis was to identify conflict-related signals within each task. To achieve this, we trained a linear classifier to distinguish between conflict and non-conflict trials separately for each task. This analysis was performed at each time point across the trial. As shown in Figure 2, the classifier successfully differentiated between conflict and non-conflict trials. Statistical analyses revealed the following significant clusters: (i) 96–1396 ms for the change detection task; (ii) smaller clusters ranging 124-188 ms, and a sustained cluster between 224–1372 ms for the Simon task; (iii) 480–1112 ms for the Stroop naming task; (iv) smaller clusters between 720-1516 ms and a sustained cluster ranging 1524–1996 ms for the Stroop reading task. Figure 2 also highlights the range in which 95% of the response times for conflict and non-conflict trials occurred. Although there is some overlap between these time windows and the significant clusters, it is unlikely that response time differences between conflict and non-conflict trials drive these decoding effects. This assertion is supported by the topographical maps for these critical time windows, which highlight a predominantly centro-frontal localization of the effect. Notably, these maps closely resemble those reported in the existing literature (Gajewski & Falkenstein, 2015; Heidlmayr et al., 2020; Schneider et al., 2012).

2.2.Successful within-task decoding – evidence from the frequency domain

In a second step, we implemented an alternative within-task decoding analysis, which uses power values from different frequencies as a feature alongside electrodes. We ran a fast Fourier transform on the 0-1000 ms window following stimulus presentation and obtained power values for the frequency range between 1-50 Hz. We implemented this second within-task decoding procedure to determine whether power values from specific frequency ranges significantly contribute to decoding accuracy (Hanslmayr et al., 2008; Nigbur et al., 2011). Additionally, eliminating the time dimension from the analysis has the advantage of being less susceptible to response times differences between conflict and non-conflict trials. Within each participant, the analysis resulted in a single decoding accuracy value.

To assess the statistical reliability of the results, we generated a null distribution of decoding accuracies by randomly shuffling conflict labels within each participant. The mean decoding accuracy was subsequently compared to the null distribution to determine its percentile rank. A value above the 95th percentile indicated significant above-chance decoding accuracy, while a value below this threshold was considered evidence for chance-level performance, supporting the null hypothesis. We obtained the following results: for the Simon, change detection, and Stroop naming tasks, the mean decoding accuracy was at the 100th percentile of the null distribution, demonstrating robust evidence for above-chance decoding performance (Figure 3). In contrast, for the Stroop reading task, the decoding accuracy was at the 67th percentile, providing evidence that the classifier could not reliably differentiate between conflict vs. non-conflict trials (Figure 3).

As shown in Figure 3 (left panels), the null distributions do not center around 0.50 but instead fall consistently above 0.50 across all four distributions. This pattern aligns with prior research suggesting that classification accuracies under the null hypothesis are not symmetrically distributed around chance (Allefeld et al., 2016).

Finally, we also conducted a searchlight analysis to examine whether specific frequency bands contributed more significantly to the decoding results. The analysis revealed that the highest decoding accuracy consistently occurred in the theta frequency range (3–7 Hz), which aligns with previous findings (Hanslmayr et al., 2008; Nigbur et al., 2011). Moreover, the

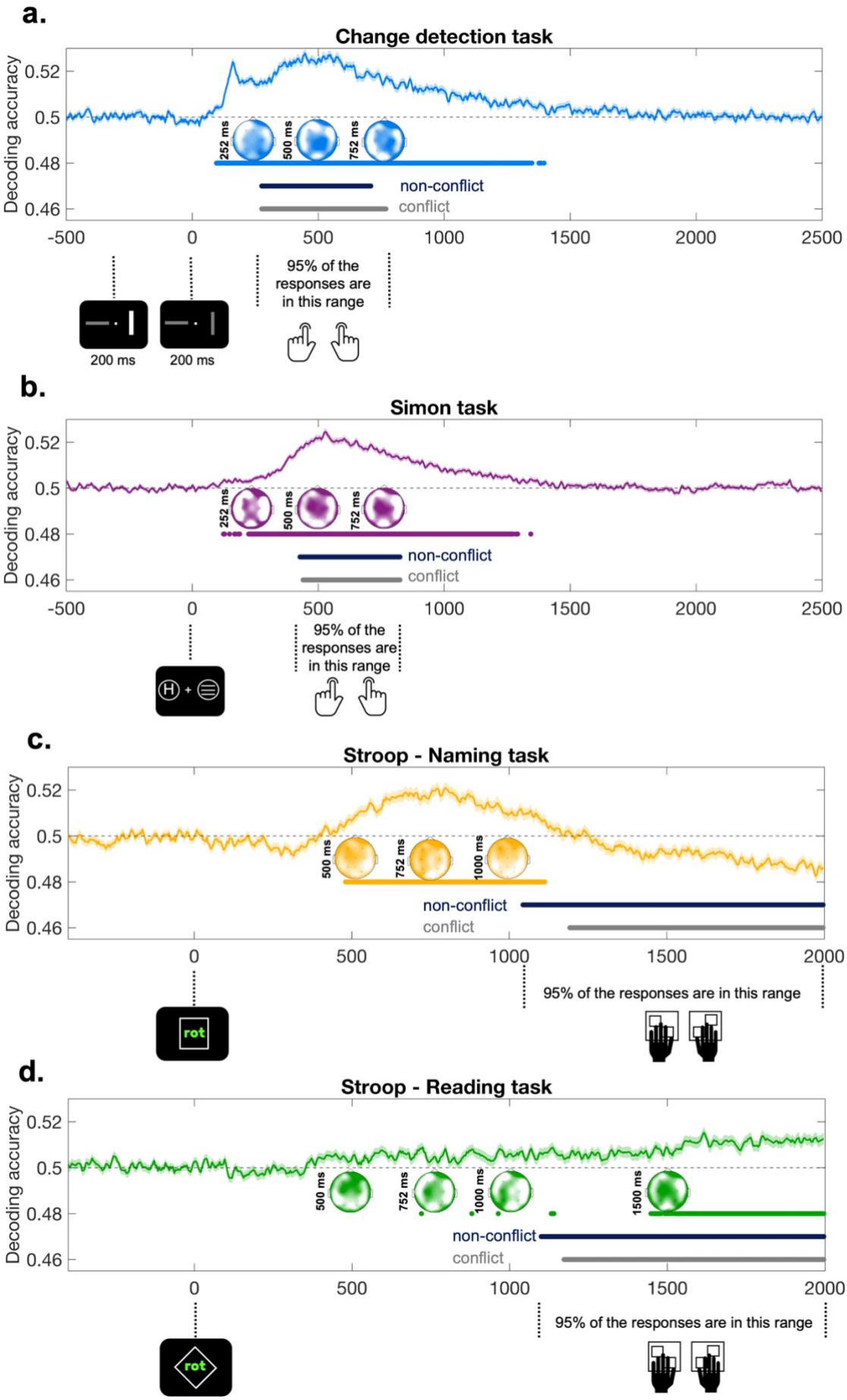

Figure 2. Decoding accuracy across time within task procedures for the (a) change detection task, (b) Simon

task, and (c, d) Stroop tasks. Dashed lines at 0.5 indicate chance level, while the shaded area around the average decoding accuracy represents the standard error of the mean. Blue, purple, yellow, and green dotted lines denote significant clusters identified through statistical analysis. Black and gray dotted lines indicate the time ranges during which 95% of the response times for conflict and non-conflict conditions occur. Each time point is annotated with the task-specific events. The topographical maps within each task panel were derived from searchlight analyses conducted at the specific time points indicated next to each map. The decoding accuracy limits for the topographical maps are as follows: (a) Change detection task: 0.50–0.514; (b) Simon task: 0.50–0.515; (c) Stroop naming task: 0.50–0.508; (d) Stroop reading task: 0.50–0.508.

topographical representation of decoding accuracies in the theta-band also revealed that these effects are maximal at fronto-central regions.

Overall, the results from both procedures demonstrated that, within each task, conflict and non-conflict trials exhibit distinct EEG patterns, allowing for successful classification. The only exception was the Stroop reading task. However, previous research suggests that the reading task does not involve the same degree of conflict as the naming task, potentially accounting for the observed outcome (Van Maanen et al., 2009). Additionally, the searchlight analysis revealed that theta frequency power plays a crucial role in decoding accuracy, with its effects exhibiting a fronto-central topographical distribution (Hanslmayr et al., 2008; Nigbur et al., 2011).

2.3. Non-generalizable conflict signal across tasks – evidence from cross-task decoding

The cross-task decoding analysis was conducted to determine whether neural patterns associated with conflict processing generalize across different cognitive tasks. Notably, the Stroop reading task was excluded from this set of analyses due to its lack of robust evidence for within-task decoding. The first approach involved a pairwise decoding procedure, in which a classifier was trained on one task and tested on another one. Each task served once as a training dataset and once as a testing dataset. The decoding and statistical procedures were identical to those used in the within-task analyses described in Section 2.2, with both channel and frequency information between 1–50 Hz serving as input features. As shown in Figure 4A, the results of this analysis revealed that the mean decoding accuracy values did not deviate from chance level, as indicated by the percentiles at which the mean decoding accuracy values are situated relative to the null distribution: (a) 4.99th percentile for change detection-Simon task; (b) 84.15th percentile for change detection-Stroop Naming task; (c) 4.90th percentile for Simon-change detection task; (d) 59.92th percentile for Simon-Stroop naming task; (e) 14.72th percentile for Stroop naming-change detection tasks; (f) 56.29th percentile for Stroop naming-Simon task. Overall, these results suggest evidence for a lack of conflict signal generalizability across tasks.

Building on the within-task results, which suggested that decoding accuracy might be driven by theta-band power (3–7 Hz; cf., Hanslmayr et al., 2008; Nigbur et al., 2011), we refined the analysis by restricting input features to this frequency band. However, as illustrated in Figure 4b, this adjustment produced the same pattern of results: evidence was found for chance-level decoding performance across all comparisons: (a) 44.60th percentile for change detection-Simon task; (b) 49.26th percentile for change detection-Stroop Naming task; (c) 16.08th percentile for Simon-change detection task; (d) 10.62th percentile for Simon-Stroop naming task; (e) 85.23th percentile for Stroop naming-change detection tasks; (f) 77.67th percentile for Stroop naming-Simon task.

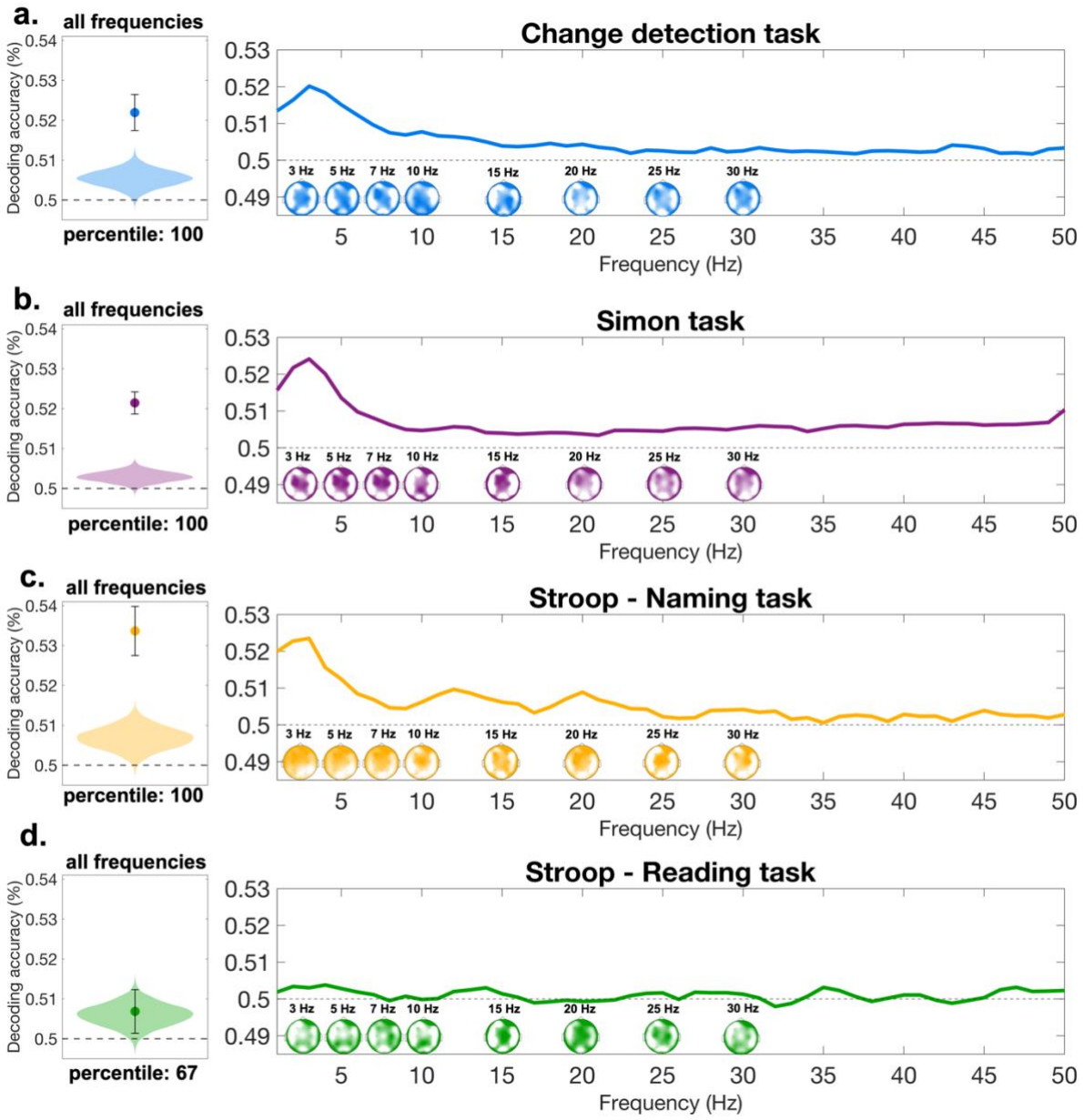

Figure 3. **Within-task decoding based on frequency-domain information**. Panels (a–d) show the results of the second within-task decoding procedure performed on power values between 1–50 Hz. The left-side panels display the comparison of mean decoding accuracy relative to the null distribution. The dashed gray line represents chance level, while the violin plot illustrates the null distribution generated by permuting conflict labels within each participant, with 10,000 permutations randomly sampled and averaged. As explained in Section 2.2, the null distribution values are not symmetrically centered around the chance level. The dot represents the mean decoding accuracy, and the error bar indicates the confidence intervals of the mean. For panels (a–c), the average decoding accuracy corresponds to the 100th percentile, while in panel (d), it falls at the 67th percentile. The right-side panels (a–d) depict the decoding accuracy from the searchlight analysis across frequency and electrode space. In the frequency representation, decoding accuracy values were averaged across all electrodes. The limits of the topographical maps are not uniform and vary across different maps. The minimum is at 0.50 and the maximum ranges between 0.503-0.51.

1

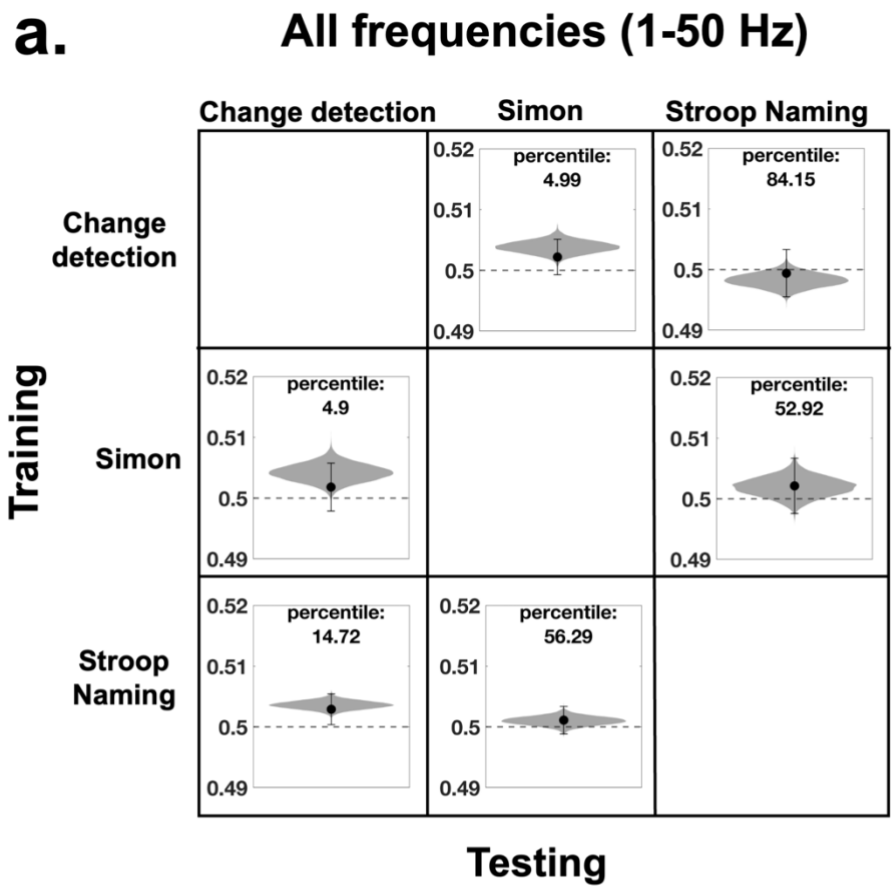

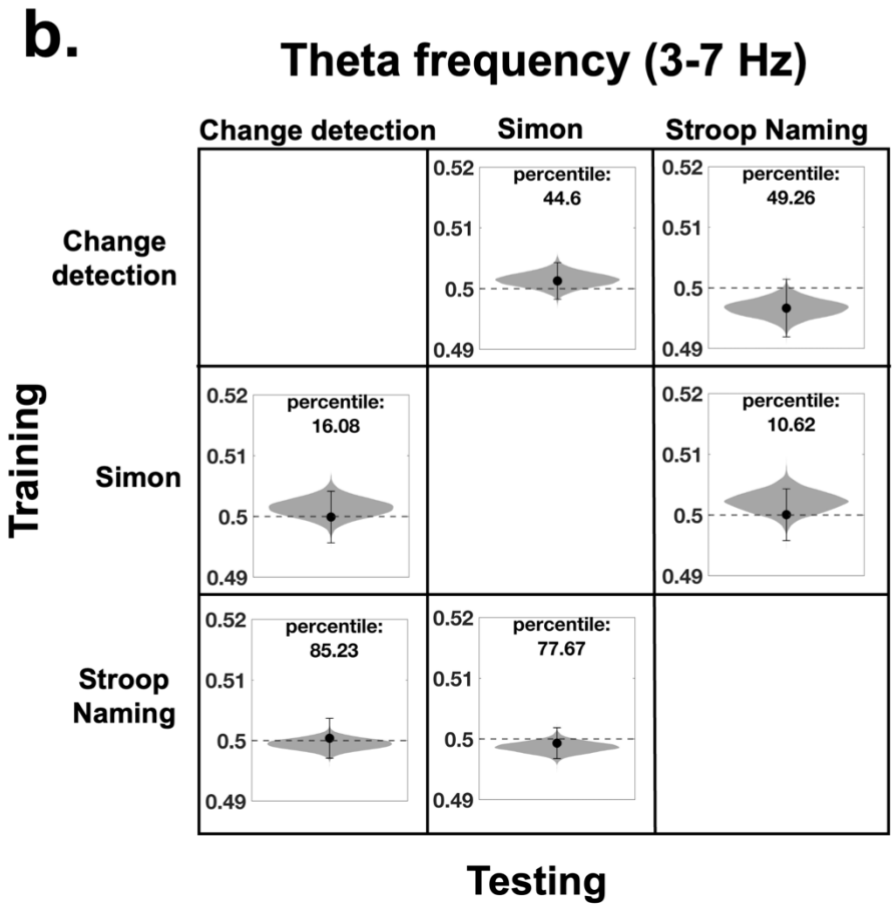

Figure 4. Cross-task decoding results. Both panels display the comparison of mean decoding accuracy relative to the null distribution across different training-testing pairs. Additionally, each sub-figure contains the percentile, where the mean decoding accuracy falls relative to the null distribution. Panel (a) represents results across all frequency ranges, and panel (b) focuses on the theta frequency range (3–7 Hz). The dashed gray line represents chance level, and the violin plot illustrates the null distribution generated by permuting conflict labels within each participant, with 10,000 permutations randomly sampled and averaged. As explained in Section 2.2, the null distribution values are not symmetrically centered around the chance level. The dot represents the mean decoding accuracy, and the error bar indicates the 95% confidence intervals of the mean.

To further test the robustness of these findings, we employed a third approach: a leave-one-task-out decoding procedure. In this method, a linear model was trained on all tasks except one, which was then used as the testing set. This approach was chosen to construct a more robust model, potentially better suited to detect a task-general conflict processing signal. The statistical procedure was identical to that used in the within-task analyses described in Section 2.2. Specifically, we constructed a null distribution and identified the percentile at which the average decoding accuracy was located. If this percentile fell below the 95th, we interpreted it as support for the null hypothesis. Conversely, percentiles above the 95th were taken as evidence of significantly above-chance decoding performance. The results corroborated the earlier findings: cross-task decoding accuracy remained at chance level, providing strong evidence for the null hypothesis. Specifically, the average decoding accuracy was positioned at the 86.97th percentile of the null distribution.

In summary, these results demonstrate that the conflict signal identified in the within-task decoding procedure does not generalize across tasks. This conclusion was robust, as it was supported by three distinct decoding approaches. We interpret these findings as evidence for our second hypothesis, which posits that, at the neural level, conflict processing and control are supported by multiple conflict-specific modules.

3. Discussion

The primary aim of the current study was to investigate whether conflict processing is governed by (i) a domain-general neural mechanism; (ii) multiple conflict-specific modules; or (iii) it is best explained by a hybrid model. To explore this, we examined whether a linear classifier could distinguish conflict from non-conflict trials based on EEG data across three distinct conflict tasks. Analyses were performed both within each task as well as across tasks. A key strength of the latter approach lies in its ability to bypass assumptions about specific neural components or regions shared across tasks (Grootswagers et al., 2017; Hebart & Baker, 2018). Instead, the method leverages the classifier's capacity to detect regularities in the data that might reflect task-independent conflict processing. By focusing on data-driven patterns, this study offers a novel approach to probing the generalizability of conflict signals, contrasting with prior research that often relies on predefined neural markers or brain regions of interest. Another distinctive aspect of this work is the dataset used for these analyses. Unlike most prior studies, which often rely on smaller or less diverse samples, this study drew on a large, representative sample of 507 individuals aged from 20 to 70 years. This large and representative sample enhances the generalizability of our findings, providing insights into conflict processing across a wide cross-section of the population. The size and diversity of this dataset mark a significant methodological advance for robust and reproducible investigations of conflict processing and control and its neural correlates.

Our findings revealed that the classifier reliably distinguished conflict from non-conflict trials across all tasks, except for the Stroop Reading task. These results align with prior research

highlighting distinct neural signatures of conflict processing and control. Specifically, the fronto-central N2 component has been consistently linked to conflict monitoring in Simon, Stroop, and change detection tasks (Gajewski & Falkenstein, 2015; Heidlmayr et al., 2020; Wascher & Beste, 2010). The parietal P3 component is another EEG correlate, whose modulation has been frequently shown in conflict tasks (Ila & Polich, 1999; Leuthold, 2011; Polich, 2007). Additionally, theta-band oscillatory activity (~3–7 Hz) has also been strongly associated with conflict resolution, particularly in Stroop and Simon tasks (Hanslmayr et al., 2008; Nigbur et al., 2011). Consistent with these findings, our searchlight analysis found that within-task decoding accuracy peaked at 3 Hz and extended across the theta range. Finally, the weaker conflict signal in the Stroop Reading task is in line with previous findings suggesting lower levels of conflict compared to the color-naming variant (Van Maanen et al., 2009). Together, these results provide robust evidence that conflict processing can be neurally tracked within each task, with components such as the N2, P3, and theta oscillations likely underlying the successful decoding.

Despite evidence for successful within-task decoding, our cross-task decoding analyses revealed that conflict signals do not generalize across tasks. Notably, this finding was robust and consistently observed across three different cross-task procedures. This supports the *perspective of multiple conflict-specific modules* and suggests that the neural mechanisms underlying conflict processing are not domain-general but are orchestrated by neural sub-modules tailored to handle task-specific conflict resolution strategies. Our results also exclude the possibility of a hybrid model, as we did not find evidence for above-chance decoding accuracy between the change detection and any other task. Our results align with frameworks suggesting that conflict processing and control operate across various levels of the brain's processing hierarchy (Egner, 2008). Specifically, the level at which conflict processing occurs depends on the nature of the information involved. For example, resolving a conflict between visual features engages the visual cortex, whereas resolving a motor or semantic conflict involves higher-level brain regions. Additionally, it is plausible that conflict processing at different cortical levels also follows a distinct temporal profile. For example, conflict between low-level visual features may be detected and processed earlier than conflict between perceptual and semantic information. This suggests that the conflict signal in different tasks is not only linked to activations in distinct brain regions but also follows different temporal dynamics. Overall, this suggests that the brain flexibly adjusts its conflict resolution strategies according to the task demands, utilizing specialized neural resources to resolve different conflict types.

Our results are also in line with a broader framework, according to which conflict processing emerges from interactions within a widespread network of brain regions that vary in both location and function (Zink et al., 2021). This perspective acknowledges the role of the anterior cingulate cortex and prefrontal cortex as part of this network but does not assign them exclusive responsibility for conflict processing and control. Crucially, the emphasis of the model is on the role of connectivity patterns within the network. While different types of conflict may activate overlapping brain regions, their specific functions are shaped by unique connectivity patterns (Zink et al., 2021). These differences in connectivity could explain the observed lack of cross-task decoding, as each task may rely on unique patterns of interaction within the network to resolve conflict (Zink et al., 2021).

While our results point to the dynamic interactions within a distributed network of brain regions involved in conflict processing, they also raise important questions about the concept of domain-general conflict processing and control. If conflict resolution depends on specialized

connectivity patterns that vary depending on the task, the idea of a unified, task-independent network with consistent properties becomes increasingly difficult to support. This debate is already prominent among researchers studying the psychometric properties of cognitive control, with evidence suggesting the absence of a latent factor for domain-general control (Oberauer, 2024; Von Bastian et al., 2020). Our findings contribute to this debate by providing neural evidence that conflict processing and cognitive control are not governed by a single, domain-general network but are instead driven by specialized connectivity patterns unique to each task.

To summarize, we investigated whether the neural mechanisms underlying conflict processing are domain-general, conflict-specific, or driven by a hybrid architecture involving both domain-general and domain-specific modules. We analyzed EEG data from 507 participants who completed three conflict tasks: a change detection task, the Simon task, and the Stroop task. Our results showed that while conflict signals could be reliably tracked within each task, they did not generalize across tasks, as evidenced by chance-level cross-task decoding results. These findings support the notion of multiple conflict-specific modules orchestrating conflict processing and control in the brain, consistent with our second prediction. Overall, these results contribute to ongoing debates about cognitive control by suggesting that conflict processing and control relies on specialized neural systems tailored to task-specific demands.

4. Methods

4.1. Participants

The present study utilized data collected within the ongoing Dortmund Vital Study (Clinicaltrials.gov NCT05155397; see Gajewski et al., 2022). At the time the current analyses were conducted, data had been collected from 614 participants. The exclusion criteria of the Dortmund Vital Study included no history of significant medical conditions, including (i) neurological disorders (e.g., dementia, Parkinson's disease, or stroke); (ii) cardiovascular diseases; (iii) bleeding disorders; (iv) cancer; (v) psychiatric conditions (e.g., schizophrenia, obsessive-compulsive disorder, anxiety disorders, or severe depression); (vi) eye conditions such as cataracts, glaucoma, or blindness. Additionally, participants with a history of head injuries, surgeries, implants and those with a reduced physical fitness or mobility were excluded. Finally, participants taking psychotropic drugs or neuroleptics were omitted from the study. However, individuals taking medications such as blood thinners, hormones, antihypertensives, or cholesterol-lowering drugs were eligible for inclusion. All participants had normal or corrected-to-normal vision and hearing.

Originally, data were collected from 614 participants, but 107 participants were excluded for various reasons; Sixty participants did not attend the second experimental session required to complete the Stroop task. Twenty-one participants had excessively noisy EEG recordings for at least one task, rendering their data unusable. Eleven participants failed the Ishihara color test, and three had vision impairments. One participant could not complete testing due to health issues, and five were excluded for not being able to complete the tasks. Additionally, two participants were excluded due to technical issues encountered during their experimental sessions. Finally, the data from four participants were excluded because they missed too many trials during the Simon task, rendering their EEG data unsuitable for the decoding analyses. The final sample included 507 participants (320 females, 187 males, age range: 20-70 years, M_{age} = 43.58, SD_{age} = 14.09).

All participants provided written informed consent prior to participation, and the study adhered to the ethical principles outlined in the Declaration of Helsinki. Ethical approval was obtained from the local ethics committee of the Leibniz Research Centre for Working Environment and Human Factors, Dortmund, Germany (approval number: A93). The four tasks included in the current study were completed in two different experimental sessions that spanned two days. Participants were compensated with 160 Euros for these two sessions.

4.2. Experimental procedure

Participants completed computer-based cognitive tasks, including a change detection task (Wascher & Beste, 2010), a Simon task (Simon, 1969), and a Stroop task (Stroop, 1935). The change detection and Simon tasks were administered on the first day, whereas the Stroop task was conducted in a separate session on a different day. EEG signals were recorded throughout the completion of these tasks.

4.2.1. Technical set-up – first session

Tasks were displayed on a 32-inch VSG monitor (Display++ LCD, M0250 & M0251) with a resolution of 1920×1080 pixels and a refresh rate of 100 Hz. Manual responses were captured using force-sensitive handles. The stimuli and presentation sequence were created using the FreePascal software. EEG data were collected using an Ag–AgCI active electrode EEG system (actiCap; Brain Products GmbH). The signal was sampled at a rate of 1000 Hz and filtered in real time with a 200 Hz low-pass filter. A 64-channel cap was used for data acquisition, with the FCz electrode serving as the reference electrode and Afz as the ground electrode.

4.2.2. Technical set-up – second session

On the second day, participants performed the tasks on a 17-inch monitor (refresh rate: 100 Hz, resolution: 640 × 480 pixels) and were seated ~70 cm away from the screen. For recording the EEG data, a 32-channel EEG system equipped with Ag–AgCl active electrodes (BioSemi B.V.) was utilized, with data sampled online at 2048 Hz. The BioSemi system incorporates a Common Mode Sense (CMS) active electrode and a Driven Right Leg (DRL) passive electrode, which together establish a feedback loop to regulate the subject's average potential. The reference and ground electrodes are included within this CMS and DRL loop. Electrode placement followed the international 10–20 system, with impedances maintained below 10 kΩ during both experimental sessions.

4.2.3. Change detection task

Participants were shown a display (luminosity: 20cd/m^2) with two bars (size: 1.35°×0.56° visual angle; color: CIE1931: 0.287, 0.312, 10-50 cd/m^2, where the last parameter has been varied between 10-50). One of the bars was always on the left, while the other on the right of a central fixation dot (size: 0.3°×0.3°; distance between fixation dot and bar: 1.3° visual angle). After 50 milliseconds, a second display appeared introducing either a luminance change, an orientation change, or both. Luminance changes occurred either from 10 to 50 cd/m^2 or from 50 to 10 cd/m^2. Similarly, orientation changes could switch from horizontal to vertical or from vertical to horizontal (Wascher & Beste, 2010). Participants' task was to indicate, via a left- or right-hand button press, whether the luminance change occurred on the left or right side. Importantly, the luminance and orientation changes could appear either together or separately. Trials were categorized as: (i) non-conflict trials, where only a luminance change occurred, or a luminance change occurred along with an orientation change in the same bar; (ii) conflict trials, in which the luminance change occurred in one bar while the orientation change occurred in the other bar.

4.2.4. Simon task

Trials in the Simon task began with a central fixation cross (size: 0.3°×0.3°) and two placeholder dots (size: 0.15°×0.15°), one on each side of the fixation displayed for a variable interval between 500 and 800 milliseconds (background color: CIE1931: 0.287, 0.312, 10). Following this, participants were shown a stimulus display consisting of two shapes on either side of the fixation cross (distance between shape and central fixation: 2° visual angle). Participants were instructed to press a button when circles appeared and to withhold their response when a diamond was present. For the current study, we only consider trials, in which a response had to be made. Within the circles (diameter in visual angles: 1.1°), letters could be displayed, always appearing on one side of the fixation cross, while the other shape contained three horizontal lines (size of each line: 0.45°×0.07° visual angle) as a placeholder (color: CIE1931: 0.287, 0.312, 80). If participants saw the letter "H" (size: 0.536°×0.474° visual angle) they were supposed to respond with one hand (e.g., left), and if they saw the letter "N" (size: 0.495°×0.474° visual angle) they were required to respond with the other hand (e.g., right). Importantly, trials were categorized as: (i) non-conflict trials when the letter that instructed the participant to press the button with a particular hand (e.g., left) appeared on the corresponding side (e.g., left); (ii) conflict trials when the letter instructing the participant to press with a specific hand appeared on the opposite side (e.g., the letter for the left hand was on the right side).

4.2.5. Stroop task

The task was divided into two main blocks. In the first block, participants' task was to indicate the word's meaning (i.e., read the color word), while in the second block, they had to report the color of the ink, in which the word is printed. The trial started with a cue (square or diamond, size: 0.33°×3.03° visual angle) indicating whether it is a color reading or a color naming task. Following a 1000 ms inter-stimulus-interval, participants were displayed a color word (size: 0.57°×0.82° visual angle). The stimuli consisted of the German words "rot," "grün," "gelb," "blau" for "red," "green," "yellow" and "blue" each displayed in one of these four colors. The color of the presented words was either compatible or incompatible with the word's meaning. Half of the trials were compatible (e.g., the word "red" displayed with red ink–non-conflict trials), and the other half were incompatible (e.g., the word "red" in green color – conflict trials). To respond, participants used four buttons, each of which had an assigned color that was learnt before starting the session. For responses, the index and middle fingers of both hands were used. The color-button assignment was the same for all participants. Participants had 2500 milliseconds to respond. At the end of the trial, they received feedback: a plus sign for correct responses and a minus sign (size: 0.82°×0.82° visual angle) for incorrect responses. The response-cue interval was 1300 milliseconds and included the response feedback and a feedback delay. The instruction encouraged both quick and accurate responses.

4.3. Data analyses

4.3.1. EEG preprocessing

Given the robustness of multivariate methods to noise (Carlson et al., 2020) minimal preprocessing was performed. Data was high-pass and low-pass filtered using a Hamming windowed sinc FIR filter and then downsampled to 250 Hz. For each task, epochs time-locked to the target stimulus were created: (i) perceptual discrimination: -500 to 2800 ms; (ii) Simon: -500 to 2500 ms; (iii) Stroop: -400 to 2000 ms. At the end, baseline removal (0–200 ms) was applied. Preprocessing was conducted using functions from the EEGLAB toolbox (v2024.0; (Delorme & Makeig, 2004) implemented in MATLAB.

4.3.2. Decoding analyses & statistics

To address the main research question, multivariate decoding analyses were performed using the CoSMoMVPA toolbox (Oosterhof et al., 2016) implemented in MATLAB. For all analyses, the classifier was trained and tested to distinguish between conflict and non-conflict trials. Therefore, the chance level was always set to 0.5 (i.e., 50%). Regularized linear discriminant analysis classifiers were employed. To ensure consistency and comparability of results, each dataset was standardized to include a common set of electrodes across all participants and sessions. Trials where participants failed to respond within the time limit were excluded.

4.3.2.1. Within-task decoding – time domain analysis

As the first step in the analysis, we performed within-task decoding, where the classifier was both trained and tested using trials from the same task. We employed a 10-fold cross-validation approach, training the classifier on 90% of the data and testing it on the remaining 10%. This process was repeated across all folds, ensuring each data segment served as the test set once. To maintain class-balance, the `cosmo_balance_partitions` function was used to ensure equal representation of conflict and non-conflict trials in both the training and testing sets. The classifier was trained and tested independently at each time point, providing precise temporal resolution of decoding accuracy (Grootswagers et al., 2017). For each time point, decoding performance was calculated as the proportion of correctly classified trials, reflecting the classifier's ability to differentiate between conflict and non-conflict conditions. We also performed a searchlight analysis. Here, we used electrode values as features, so the analysis was performed individually for each electrode and timepoint, yielding topographical maps at the following key timepoints: 252, 500, 752, 1000, 1500 ms. Statistical analyses were conducted using the `cosmo_montecarlo_cluster_stat`, which incorporates Threshold-Free Cluster Enhancement (Smith & Nichols, 2009) and Monte Carlo-based permutation testing (Maris & Oostenveld, 2007) to account for multiple comparisons (Oosterhof et al., 2016).

4.3.2.2. Within-task decoding – frequency-domain analysis

In a second step, we implemented an alternative within-task decoding analysis, which uses power values from different frequencies as a feature alongside electrodes. We implemented this second within-task decoding procedure to determine whether power values from specific frequency ranges significantly contribute to decoding accuracy (Hanslmayr et al., 2008; Nigbur et al., 2011). This approach excludes the temporal dimension by applying a fast Fourier transform to the 0–1000 ms window following stimulus presentation, converting raw EEG signals into power at each frequency value. Power values within the 1–50 Hz range were extracted and used as features in the decoding analysis alongside electrode data, resulting in a single decoding accuracy value per participant. As in the previous decoding analysis, we employed a 10-fold cross-validation procedure, ensuring equal representation of conflict and non-conflict trials in both training and testing sets. Before running the decoding procedure, values underwent z-transformation. Finally, classifier performance was quantified as the proportion of correctly classified trials. For the searchlight analysis, we followed the same procedure, with one key difference: instead of using electrodes and frequency values as features, the analysis was conducted separately for each electrode and frequency combination. First, we plotted the average decoding accuracy across all electrodes for the frequency range 1-50 Hz. Additionally, topographies are also shown for a set of key frequencies: 3, 5, 7, 10, 15, 20, 25, 30 Hz.

To evaluate the statistical reliability of the results, we generated a null distribution for each task. Conflict and non-conflict labels were randomly permuted 100 times per participant,

generating 100 decoding accuracy values per participant. From these, one decoding accuracy value per participant was randomly selected, and the mean decoding accuracy across participants was calculated (Stelzer et al., 2013). This process was repeated 10,000 times to construct the null distribution. Finally, we compared the observed mean decoding accuracy to this null distribution, determining the percentile at which it fell. A percentile value falling below the 95th percentile is interpreted as evidence for the null hypothesis, while values above 95 represent evidence for significant above-chance decoding.

4.3.2.3. Cross-task decoding – frequency-domain analysis

The cross-task decoding procedure was designed to examine whether neural patterns associated with conflict and non-conflict trials could generalize across different cognitive tasks. Notably, the Stroop reading task was excluded from this set of analyses due to its lack of robust evidence for within-task decoding. The cross-task decoding procedure was modeled after the steps used in the within-task decoding analysis applied to the frequency domain. Specifically, we applied a Fast Fourier Transform to the 0–1000 ms window following the stimulus presentation and extracted power values within the 1–50 Hz range, which were used as input for classification. Data averaging was performed to enhance the signal-to-noise ratio and ensure a sufficient number of super-trials for robust modeling, generating 200 super-trials from the training set and 200 from the testing set, with conflict and non-conflict trials equally represented. Three different approaches were employed in this analysis: (i) Pairwise cross-task decoding (1–50 Hz): All tasks were used as both training and testing datasets, with power values between 1–50 Hz included. (ii) Pairwise cross-task decoding (4–7 Hz): All tasks were used as both training and testing datasets, but only power values within the 4–7 Hz range were included. (iii) Leave-one-out model: Training was conducted using three out of four tasks, with testing performed on the remaining task. Importantly, the leave-one-task-out procedure chosen to construct a more robust model, was potentially better suited to detect a task-general conflict processing signal. The procedure was comparable to pair-wise cross-task decoding, with trials from the training tasks stacked together and trials from the test task evaluated independently. The same statistical procedure described in Section 4.3.2.2 was applied to this analysis.

Author contribution – CrediT statement

M.S.: Conceptualization, Data Curation, Software, Methodology, Validation, Formal Analysis, Visualization, Project Administration, Writing – Original Draft, Writing – Review & Editing. T.G.: Conceptualization, Software, Methodology, Writing – Review & Editing. M.V.: Methodology, Writing – Review & Editing.

Open practices and data availability statement

The experiment was not preregistered. A sample dataset and all the scripts used for the reported analyses are publicly available on Open Science Framework (OSF): https://osf.io/ctqvy/ Access to the full dataset can be requested by contacting the Leibniz Research Centre for Working Environment and Human Factors, Dortmund, Germany.

Conflict of interest

The authors declare no competing financial interests.

Funding

This work was supported by the International Visiting Scholar Program at The MARCS Institute for Brain, Behaviour, and Development, Western Sydney University and the Australian Research Council Discovery (T.G. Early Career Researcher Award DE230100380; M.V. DP220103047).

Acknowledgments

We would like to thank Edmund Wascher, Daniel Schneider, Patrick Gajewski, Stephan Getzmann, Emad Alyan, and Stefan Arnau for their valuable input and comments. We also thank the Dortmund Vital Study team for their support: Ludger Blanke, Tobias Blanke, Claudia Brockhaus, Pia Deltenre, Barbara Foschi, Silke Joiko, Karin Lukaszewski, Carola Reiffen, and Christiane Westedt.

References

Allefeld, C., Görgen, K., & Haynes, J.-D. (2016). Valid population inference for information-based imaging: From the second-level t -test to prevalence inference. *NeuroImage*, *141*, 378–392. https://doi.org/10.1016/j.neuroimage.2016.07.040

Blais, C., & Bunge, S. (2010). Behavioral and Neural Evidence for Item-specific Performance Monitoring. *Journal of Cognitive Neuroscience*, *22*(12), 2758–2767. https://doi.org/10.1162/jocn.2009.21365

Botvinick, M. M., Braver, T. S., Barch, D. M., Carter, C. S., & Cohen, J. D. (2001). *Conflict Monitoring and Cognitive Control*.

Carlson, T. A., Grootswagers, T., & Robinson, A. K. (2020). An Introduction to Time-Resolved Decoding Analysis for M/EEG. In D. Poeppel, G. R. Mangun, & M. S. Gazzaniga (Eds.), *The Cognitive Neurosciences* (p. 0). The MIT Press. https://doi.org/10.7551/mitpress/11442.003.0075

Cespón, J., Hommel, B., Korsch, M., & Galashan, D. (2020). The neurocognitive underpinnings of the Simon effect: An integrative review of current research. *Cognitive, Affective, & Behavioral Neuroscience*, *20*(6), 1133–1172. https://doi.org/10.3758/s13415-020-00836-y

Delorme, A., & Makeig, S. (2004). EEGLAB: an open source toolbox for analysis of single-trial EEG dynamics including independent component analysis. *Journal of Neuroscience Methods*, *134*(1), 9–21. https://doi.org/10.1016/j.jneumeth.2003.10.009

Egner, T. (2008). Multiple conflict-driven control mechanisms in the human brain. *Trends in Cognitive Sciences*, *12*(10), 374–380. https://doi.org/10.1016/j.tics.2008.07.001

Egner, T., Delano, M., & Hirsch, J. (2007). Separate conflict-specific cognitive control mechanisms in the human brain. *NeuroImage*, *35*(2), 940–948. https://doi.org/10.1016/j.neuroimage.2006.11.061

Funes, M. J., Lupiáñez, J., & Humphreys, G. (2010). Analyzing the generality of conflict adaptation effects. *Journal of Experimental Psychology: Human Perception and Performance*, *36*(1), 147–161. https://doi.org/10.1037/a0017598

Gajewski, P. D., & Falkenstein, M. (2015). Long-term habitual physical activity is associated with lower distractibility in a Stroop interference task in aging: Behavioral and ERP evidence. *Brain and Cognition*, *98*, 87–101. https://doi.org/10.1016/j.bandc.2015.06.004

Gajewski, P. D., Getzmann, S., Bröde, P., Burke, M., Cadenas, C., Capellino, S., Claus, M., Genç, E., Golka, K., Hengstler, J. G., Kleinsorge, T., Marchan, R., Nitsche, M. A., Reinders, J., van Thriel, C., Watzl, C., & Wascher, E. (2022). Impact of Biological and Lifestyle Factors on Cognitive Aging and Work Ability in the Dortmund Vital Study: Protocol of an Interdisciplinary, Cross-sectional, and Longitudinal Study. *JMIR Res Protoc*, *11*(3), e32352. https://doi.org/10.2196/32352

Gratton, G., Cooper, P., Fabiani, M., Carter, C. S., & Karayanidis, F. (2018). Dynamics of cognitive control: Theoretical bases, paradigms, and a view for the future. *Psychophysiology*, *55*(3), e13016. https://doi.org/10.1111/psyp.13016

Grootswagers, T., Wardle, S. G., & Carlson, T. A. (2017). Decoding Dynamic Brain Patterns from Evoked Responses: A Tutorial on Multivariate Pattern Analysis Applied to Time Series Neuroimaging Data. *Journal of Cognitive Neuroscience*, *29*(4), 677–697. https://doi.org/10.1162/jocn_a_01068

Hanslmayr, S., Pastötter, B., Bäuml, K.-H., Gruber, S., Wimber, M., & Klimesch, W. (2008). The Electrophysiological Dynamics of Interference during the Stroop Task. *Journal of Cognitive Neuroscience*, *20*(2), 215–225. https://doi.org/10.1162/jocn.2008.20020

Hebart, M. N., & Baker, C. I. (2018). Deconstructing multivariate decoding for the study of brain function. *NeuroImage*, *180*, 4–18. https://doi.org/10.1016/j.neuroimage.2017.08.005

Heidlmayr, K., Kihlstedt, M., & Isel, F. (2020). A review on the electroencephalography markers of Stroop executive control processes. *Brain and Cognition*, *146*, 105637. https://doi.org/10.1016/j.bandc.2020.105637

Hommel, B. (2011). The Simon effect as tool and heuristic. *Acta Psychologica*, *136*(2), 189–202. https://doi.org/10.1016/j.actpsy.2010.04.011

Ila, A. B., & Polich, J. (1999). P300 and response time from a manual Stroop task. *Clinical Neurophysiology*, *110*(2), 367–373. https://doi.org/10.1016/S0168-5597(98)00053-7

Kan, I. P., Teubner-Rhodes, S., Drummey, A. B., Nutile, L., Krupa, L., & Novick, J. M. (2013). To adapt or not to adapt: The question of domain-general cognitive control. *Cognition*, *129*(3), 637–651. https://doi.org/10.1016/j.cognition.2013.09.001

Kim, C., Chung, C., & Kim, J. (2010). Multiple cognitive control mechanisms associated with the nature of conflict. *Neuroscience Letters*, *476*(3), 156–160. https://doi.org/10.1016/j.neulet.2010.04.019

Leuthold, H. (2011). The Simon effect in cognitive electrophysiology: A short review. *Acta Psychologica*, *136*(2), 203–211. https://doi.org/10.1016/j.actpsy.2010.08.001

Li, H., Liu, N., Li, Y., Weidner, R., Fink, G. R., & Chen, Q. (2019). The Simon Effect Based on Allocentric and Egocentric Reference Frame: Common and Specific Neural Correlates. *Scientific Reports*, *9*(1), 13727. https://doi.org/10.1038/s41598-019-49990-5

Li, Q., Yang, G., Li, Z., Qi, Y., Cole, M. W., & Liu, X. (2017). Conflict detection and resolution rely on a combination of common and distinct cognitive control networks. *Neuroscience & Biobehavioral Reviews*, *83*, 123–131. https://doi.org/10.1016/j.neubiorev.2017.09.032

Maris, E., & Oostenveld, R. (2007). Nonparametric statistical testing of EEG- and MEG-data. *Journal of Neuroscience Methods*, *164*(1), 177–190. https://doi.org/10.1016/j.jneumeth.2007.03.024

Nigbur, R., Ivanova, G., & Stürmer, B. (2011). Theta power as a marker for cognitive interference. *Clinical Neurophysiology*, *122*(11), 2185–2194. https://doi.org/10.1016/j.clinph.2011.03.030

Oberauer, K. (2024). The meaning of attention control. *Psychological Review*, *131*(6), 1509–1526. https://doi.org/10.1037/rev0000514

Oosterhof, N. N., Connolly, A. C., & Haxby, J. V. (2016). CoSMoMVPA: Multi-Modal Multivariate Pattern Analysis of Neuroimaging Data in Matlab/GNU Octave. *Frontiers in Neuroinformatics*, *10*. https://www.frontiersin.org/journals/neuroinformatics/articles/10.3389/fninf.2016.00027

Parris, B. A., Hasshim, N., Wadsley, M., Augustinova, M., & Ferrand, L. (2022). The loci of Stroop effects: A critical review of methods and evidence for levels of processing contributing to color-word Stroop effects and the implications for the loci of attentional selection. *Psychological Research*, *86*(4), 1029–1053. https://doi.org/10.1007/s00426-021-01554-x

Parris, B. A., Wadsley, M. G., Hasshim, N., Benattayallah, A., Augustinova, M., & Ferrand, L. (2019). An fMRI Study of Response and Semantic Conflict in the Stroop Task. *Frontiers in Psychology*, *10*, 2426. https://doi.org/10.3389/fpsyg.2019.02426

Polich, J. (2007). Updating P300: An integrative theory of P3a and P3b. *Clinical Neurophysiology*, *118*(10), 2128–2148. https://doi.org/10.1016/j.clinph.2007.04.019

Scerrati, E., Lugli, L., Nicoletti, R., & Umiltà, C. (2017). Comparing Stroop-like and Simon Effects on Perceptual Features. *Scientific Reports*, *7*(1), 17815. https://doi.org/10.1038/s41598-017-18185-1

Schneider, D., Beste, C., & Wascher, E. (2012). Attentional Capture by Irrelevant Transients Leads to Perceptual Errors in a Competitive Change Detection Task. *Frontiers in Psychology*, *3*. https://doi.org/10.3389/fpsyg.2012.00164

Schneider, D., & Wascher, E. (2013). Mechanisms of target localization in visual change detection: An interplay of gating and filtering. *Behavioural Brain Research*, *256*, 311–319. https://doi.org/10.1016/j.bbr.2013.08.046

Simon, J. R. (1969). Reactions toward the source of stimulation. *Journal of Experimental Psychology*, *81*(1), 174–176. https://doi.org/10.1037/h0027448

Smith, S., & Nichols, T. (2009). Threshold-free cluster enhancement: Addressing problems of smoothing, threshold dependence and localisation in cluster inference. *NeuroImage*, *44*(1), 83–98. https://doi.org/10.1016/j.neuroimage.2008.03.061

Stelzer, J., Chen, Y., & Turner, R. (2013). Statistical inference and multiple testing correction in classification-based multi-voxel pattern analysis (MVPA): Random permutations and cluster size control. *NeuroImage*, *65*, 69–82. https://doi.org/10.1016/j.neuroimage.2012.09.063

Stroop, J. R. (1935). Studies of interference in serial verbal reactions. *Journal of Experimental Psychology*, *18*(6), 643–662. https://doi.org/10.1037/h0054651

Van Maanen, L., Van Rijn, H., & Borst, J. P. (2009). Stroop and picture—Word interference are two sides of the same coin. *Psychonomic Bulletin & Review*, *16*(6), 987–999. https://doi.org/10.3758/PBR.16.6.987

Von Bastian, C. C., Blais, C., Brewer, G. A., Gyurkovics, M., Hedge, C., Kałamała, P., Meier, M. E., Oberauer, K., Rey-Mermet, A., Rouder, J. N., Souza, A. S., Bartsch, L. M., Conway, A. R. A., Draheim, C., Engle, R. W., Friedman, N. P., Frischkorn, G. T., Gustavson, D. E., Koch, I., … Wiemers, E. A. (2020). *Advancing the understanding of individual differences in attentional control: Theoretical, methodological, and analytical considerations*. PsyArXiv. https://doi.org/10.31234/osf.io/x3b9k

Wascher, E., & Beste, C. (2010). Tuning Perceptual Competition. *Journal of Neurophysiology*, *103*(2), 1057–1065. https://doi.org/10.1152/jn.00376.2009

Zink, N., Lenartowicz, A., & Markett, S. (2021). A new era for executive function research: On the transition from centralized to distributed executive functioning. *Neuroscience & Biobehavioral Reviews*, *124*, 235–244. https://doi.org/10.1016/j.neubiorev.2021.02.011

Zmigrod, S., Zmigrod, L., & Hommel, B. (2016). Transcranial direct current stimulation (tDCS) over the right dorsolateral prefrontal cortex affects stimulus conflict but not response conflict. *Neuroscience*, *322*, 320–325. https://doi.org/10.1016/j.neuroscience.2016.02.046

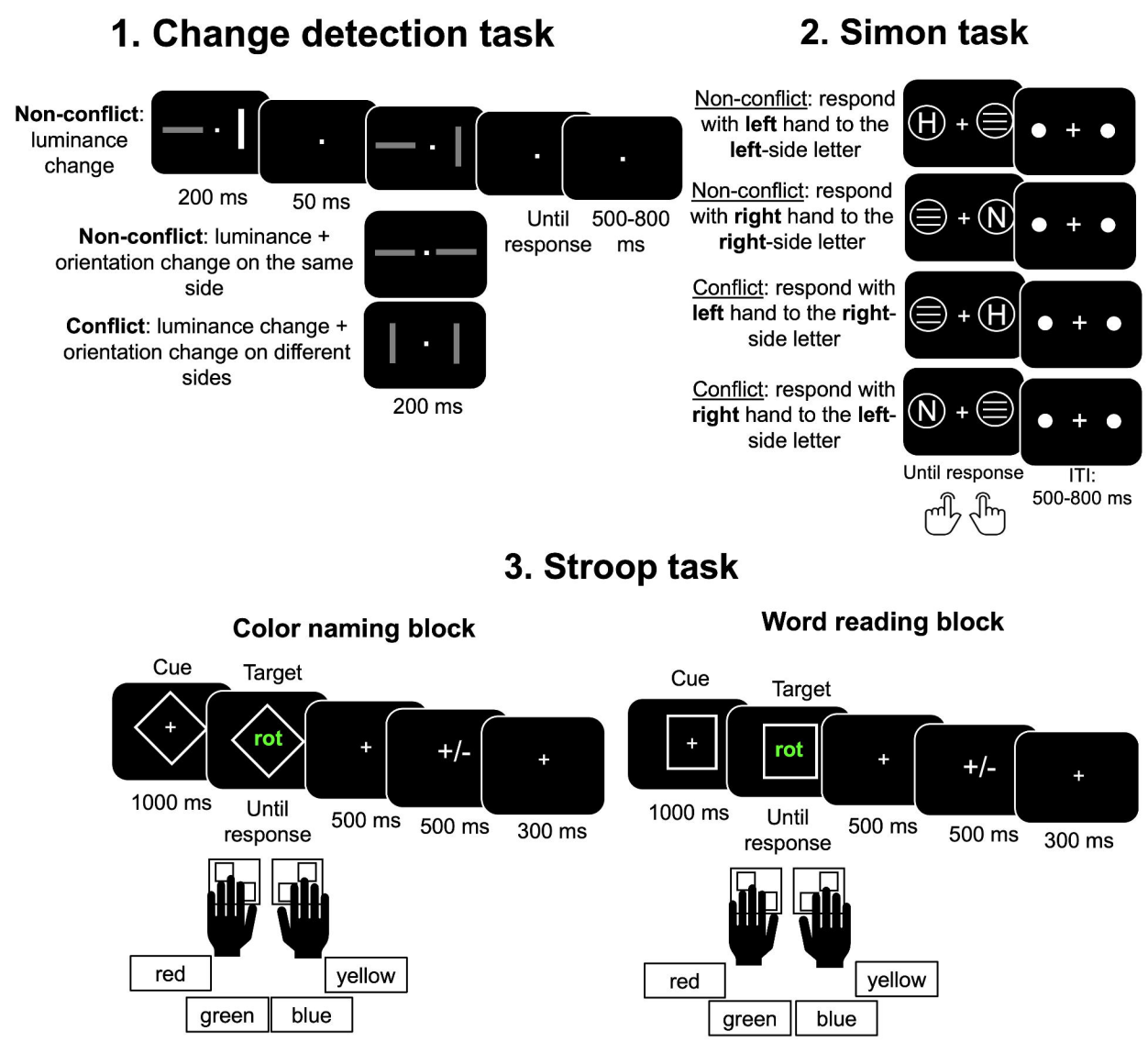
1. Change detection task
Non-conflict: luminance change
200 ms
50 ms
Until response
500-800 ms
Non-conflict: luminance + orientation change on the same side
Conflict: luminance change + orientation change on different sides
200 ms
2. Simon task
Non-conflict: respond with left hand to the left-side letter
Non-conflict: respond with right hand to the right-side letter
Conflict: respond with left hand to the right-side letter
Conflict: respond with right hand to the left-side letter
Until response
ITI: 500-800 ms
3. Stroop task
Color naming block
Cue
Target
rot
1000 ms
Until response
500 ms
500 ms
300 ms
red
yellow
green
blue
Word reading block
Cue
Target
rot
1000 ms
Until response
500 ms
500 ms
300 ms
red
yellow
green
blue

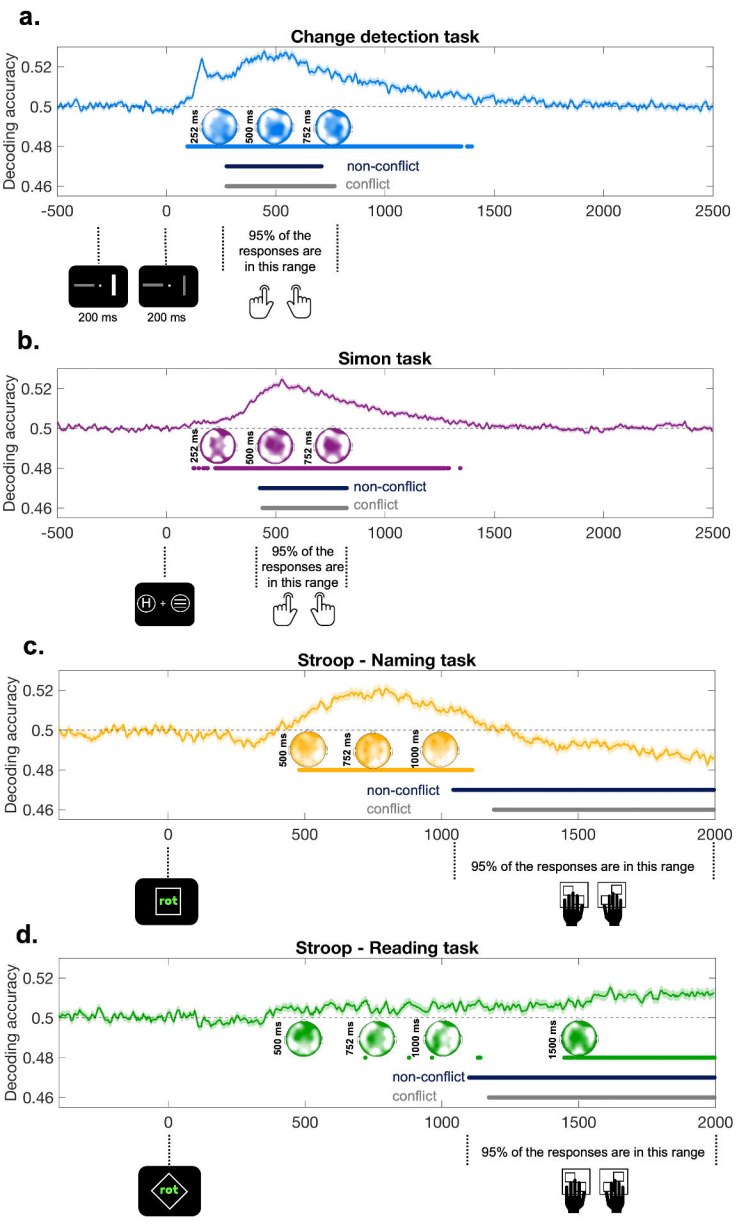
a.
Change detection task
Decoding accuracy
0.52
0.5
0.48
0.46
252 ms
500 ms
752 ms
non-conflict
conflict
-500
0
500
1000
1500
2000
2500
200 ms
200 ms
95% of the responses are in this range
b.
Simon task
Decoding accuracy
0.52
0.5
0.48
0.46
252 ms
500 ms
752 ms
non-conflict
conflict
-500
0
500
1000
1500
2000
2500
H
95% of the responses are in this range
c.
Stroop - Naming task
Decoding accuracy
0.52
0.5
0.48
0.46
500 ms
752 ms
1000 ms
non-conflict
conflict
0
500
1000
1500
2000
rot
95% of the responses are in this range
d.
Stroop - Reading task
Decoding accuracy
0.52
0.5
0.48
0.46
500 ms
752 ms
1000 ms
1500 ms
non-conflict
conflict
0
500
1000
1500
2000
rot
95% of the responses are in this range

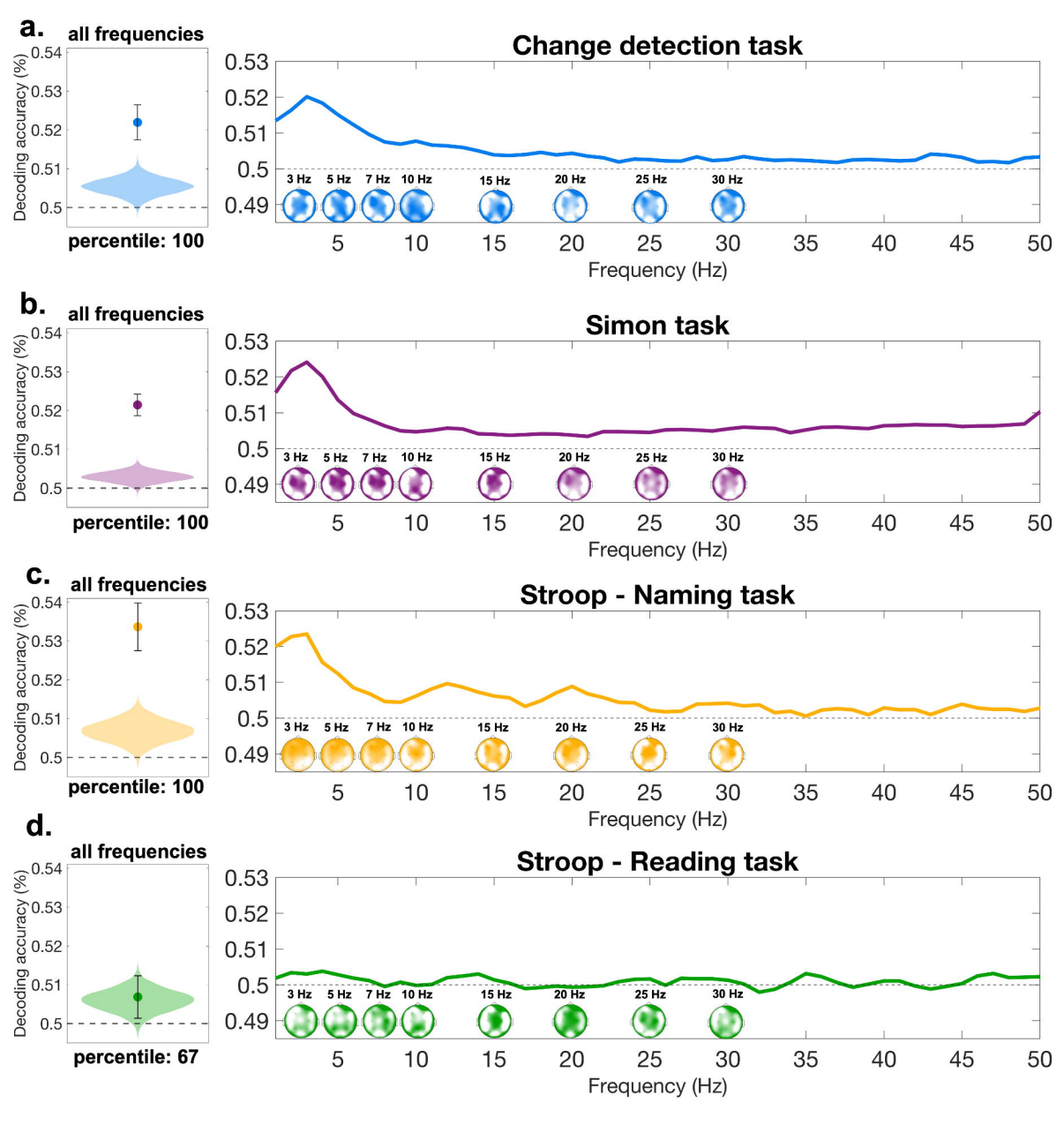
a.
all frequencies
Decoding accuracy (%)
0.54
0.53
0.52
0.51
0.5
percentile: 100
Change detection task
0.53
0.52
0.51
0.5
0.49
3 Hz
5 Hz
7 Hz
10 Hz
15 Hz
20 Hz
25 Hz
30 Hz
5
10
15
20
25
30
35
40
45
50
Frequency (Hz)
b.
all frequencies
Decoding accuracy (%)
0.54
0.53
0.52
0.51
0.5
percentile: 100
Simon task
0.53
0.52
0.51
0.5
0.49
3 Hz
5 Hz
7 Hz
10 Hz
15 Hz
20 Hz
25 Hz
30 Hz
5
10
15
20
25
30
35
40
45
50
Frequency (Hz)
c.
all frequencies
Decoding accuracy (%)
0.54
0.53
0.52
0.51
0.5
percentile: 100
Stroop - Naming task
0.53
0.52
0.51
0.5
0.49
3 Hz
5 Hz
7 Hz
10 Hz
15 Hz
20 Hz
25 Hz
30 Hz
5
10
15
20
25
30
35
40
45
50
Frequency (Hz)
d.
all frequencies
Decoding accuracy (%)
0.54
0.53
0.52
0.51
0.5
percentile: 67
Stroop - Reading task
0.53
0.52
0.51
0.5
0.49
3 Hz
5 Hz
7 Hz
10 Hz
15 Hz
20 Hz
25 Hz
30 Hz
5
10
15
20
25
30
35
40
45
50
Frequency (Hz)

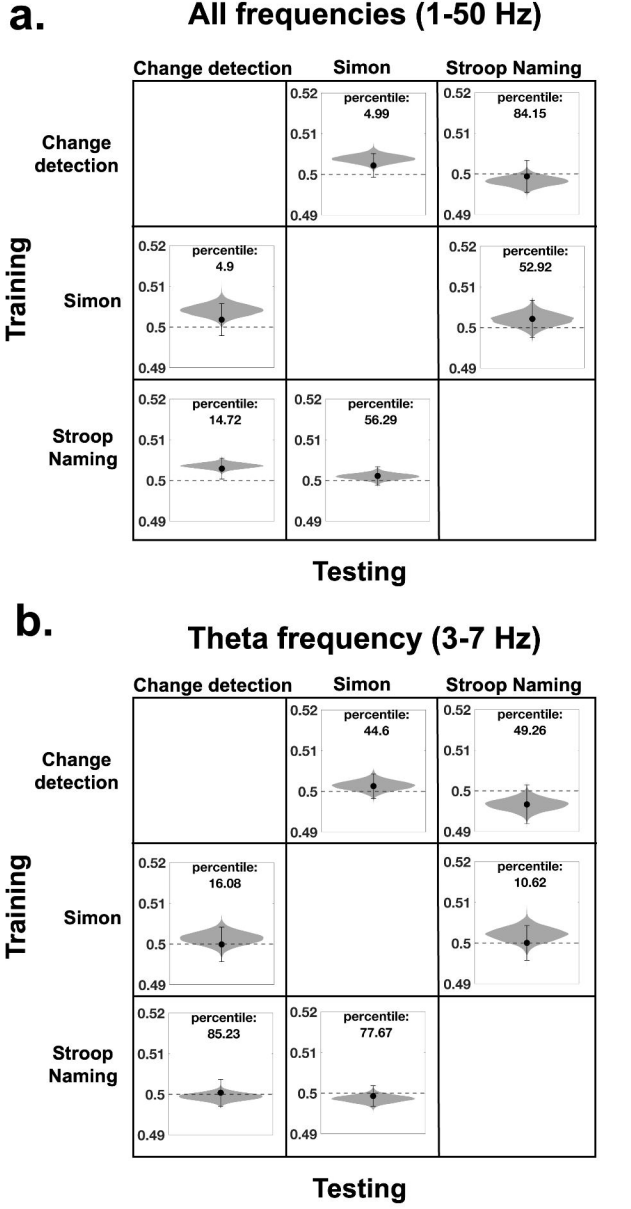
a.
All frequencies (1-50 Hz)
Change detection
Simon
Stroop Naming
Training
Change detection
Simon
Stroop Naming
Testing
percentile: 4.99
percentile: 84.15
percentile: 4.9
percentile: 52.92
percentile: 14.72
percentile: 56.29
0.52
0.51
0.5
0.49
b.
Theta frequency (3-7 Hz)
Change detection
Simon
Stroop Naming
Training
Change detection
Simon
Stroop Naming
Testing
percentile: 44.6
percentile: 49.26
percentile: 16.08
percentile: 10.62
percentile: 85.23
percentile: 77.67
0.52
0.51
0.5
0.49